symmetry

MDPI

Communication

Reaction of Triazolic Aldehydes with Diisopropyl Zinc. Chirality Dissipation versus Amplification

Oleg A. Mikhailov,[1] Elena Sh. Saigitbatalova,[2] Liliya Z. Latypova,[2] Almira R. Kurbangalieva[2,*] and Ilya D. Gridnev[1,*]

[1] N. D. Zelinsky Institute of Organic Chemistry, Leninsky prosp. 47, Moscow 119991 Russian Federation
[2] Biofunctional Chemistry Laboratory, A. Butlerov Institute of Chemistry, Kazan Federal University, 18 Kremlyovskaya Street, 420008 Kazan, Russia
* Correspondence: IDG ilyaiochem@gmail.com; ARK akurbang@kpfu.ru

Abstract: Phenomenon of Amplyfiyng Asymmetric Autocatalysis (AAA) is recently restricted to alkylation of several specific substrates with diisopropyl zinc (Soai Reaction). Targeting on the extension of the scope of this phenomenon, we studied reaction of triazolic aldehydes with diisopropyl zinc. Experiments demonstrated diversity of results involving dissipation of chirality, conserving the existent ee, and spontaneous chirality generation. Computational analysis showed that depending on the level of oligomerization of the catalyst one could expect amplification (monomeric catalyst), keeping the existing chirality (dimeric catalyst) or dissipation of chirality (tetrameric catalyst). These findings give a hope for elaborating synthetic protocols controlling chirality generation. In addition, three optically active triazolic alcohols were characterized.

Keywords: Soai reaction; chirality amplification; diisopropyl zinc; DFT computations; triazoles

1. Introduction

Discovery of autocatalytic and autoamplifying Soai reaction [1] made a strong impression on the modern chemists. Capability of a chiral catalyst to reproduce and amplify its chirality inevitably results in an aptitude of this system for a spontaneous chirality generation [2] which is extremely interesting from several points of view. First, this phenomenon is closely connected with the fundamental problem of the emergence of chiral life on the Earth [3]. Not less important are conceivable synthetic applications if the regularities of this process would become understood to a sufficient extent. Besides, the analysis of structural requirements for the reagents necessary for promoting such complicated event opens new perspective for understanding details of molecular behavior in sophisticated and challenging systems [4].

Inherently stochastic character of the spontaneous chirality generation implies exponential increase of the number of experiments required for reliable conclusion on the authentic event. However, the principal question of the authenticity of this phenomenon in a system demonstrating asymmetric autoamplification was solved positively 20 years ago in a series of publications [5-7]. On the other hand, the group of Soai provided ample evidence for the aptitude of various chiral additives to initiate the induction of chirality with the handedness determined by the structure of the inductor [8]. It is evident that both these events require the same thing, *i.e.* the presence of AAA (Amplifying Asymmetric Autocatalysis) [4].

These considerations lead to an important conclusion: if some reaction without chiral additives provides a scalemic product, we do not need to bother if it was a true absolute asymmetric synthesis observed in this particular experiment or this event was caused by the presence of tiny amounts of a chiral inductor of unspecified origin. In any case the

Citation: To be added by editorial staff during production.

Academic Editor: Firstname Lastname

Received: date
Revised: date
Accepted: date
Published: date

AAA is operating and if it would be absolutely necessary the real spontaneous chirality generation can be confirmed for this system.

Another important feature of the Soai reaction is its strict requirements to the structure of reagents. Thus, so far only diisopropyl zinc has been successfully applied as an alkylating reagent. Structures of the effective substrates are also rigorously limited by combination of pyrymidynic core, acetylenic linker and bulky terminal anchor (*t*-Bu, Me_3Si, adamantyl). These limitations arise from a sophisticated tetrameric structure of the amplifying autocatalyst [9]; any simplification of the structure leads to a considerable depletion of the performance with a notable exception of a recently reported pyridine based molecule with the same linker and anchor [10].

Numerous possibilities of the AAA are conceivable for oligomeric catalysts following Frank-Decker scheme for autoamplification or due to the reservoir effect for the monomeric catalyst [11]. Being interested in extending the structural scope of autocatalytic and autoamplifying reactions, we have launched a project for searching new examples of such transformations.

2. Materials and Methods

2.1. Experimental Details

Diisopropylzinc 1M solution in toluene (Sigma-Aldrich) was used as received without further purification. All solvents were purified and distilled by standard procedures. Analytical thin layer chromatography (TLC)was carried out on Sorbfil PTLC-AF-A-UF plates using (acetone-chloroform, 1:4) as the eluent and UV light (254 nm) as the visualizing agent. Silica gel 60A (Acros Organics, 400–230 mesh, 0.040–0.063 mm) was used for open column chromatography. Melting points were recorded with a Boëtius melting point instrument and are uncorrected. NMR spectra were measured on a Bruker Avance 300 spectrometer at 300.13 MHz (1 H) and 75.47 MHz (13 C), Bruker Avance 600 spectrometer at 600.13 MHz (1 H) and 150.90 MHz (13 C) at 20 °C in the deuterated chloroform. The chemical shifts (δ) are expressed in parts per million (ppm) and are calibrated using residual undeuterated solvent peak as an intern**al reference (CDCl 3 : δ H 7.26,** δ C 77.16). All coupling constants (J) are reported in Hertz (Hz), and multiplicities are indicated as: s (singlet), d (doublet) and m (multiplet). High-resolution mass spectra (HRMS) were obtained by lectrospray ionization (ESI) with positive (+) ion detection on a Bruker micrO-TOF–QIII quadrupole time-of-flight mass spectrometer. The ee measurement were performed by HPLC analysis. HPLC analysis was performed on an HPLC system equipped with chiral stationary phase columns (AD-H, AS-H, OD-H, OJ-H), detection at 220 or 254 nm. Synthetic procedures and characterization details for the new compounds can be found in the Supplementary Materials.

2.1. Computationall Details

Geometry optimizations were performed without any symmetry constraints (C1 symmetry) using the ωB97XD functional[1] as implemented in the Gaussian09 software package.[2] Frequency calculations were undertaken to confirm the nature of the stationary points, yielding one imaginary frequency for all transition states (TS) and zero for all minima. Constrained energy hypersurface scans were conducted to investigate the molecular reactivity and to locate viable reaction channels. Where low-lying barriers were estimated, frequency calculations were performed at the crude saddle points and the obtained force constants used to optimize the transition state structures employing the Berny algorithm [3]. All atoms were described with 6-31G** basis set in the geometries optimization and frequency calculation [4-9]. Non-specific solvation was introduced by using the SMD continuum model [10] (acetonitrile).

3. Results

2.1. Development of a Strategy for the screening of promising substrates

Despite the extensive development of various enantioselective reactions seen at present time, practically each of them requires more or less arbitrary optimization of the reaction conditions, *i.e.* structure of the catalyst, solvent, reaction temperature, pressure, additives, *etc*. Quite frequently among a dozen of chiral catalysts, each of them providing an utmost performance in some already known transformations, only one or two are really working in a newly discovered asymmetric catalytic reaction. Before these winners are actually found, the tables listing yields and ee's may look out desperately, and only the persistence in this random search may result in a happy finding.

In our case it is impossible to incorporate the same approach to each of the substrate candidates for AAA, since it would require too long time. Nevertheless, we need some more readily available results that would justify transfer of a reaction into the Step Two of the screening. We decided to check if the ability to effectuate an autocatalytic reaction can serve as such criterion without making the whole screening unreasonably tiresome.

To do this we have designed and synthesized a small series of compounds to some extent similar to the effective substrates of the Soai reaction and used them in a following trial sequence (Scheme 1,2).

3.2. Design and synthesis of the perspecvtive substrates

Looking for possible perspective substrates we were attracted by 1,2,3-triazole skeleton since it implies a possibility for introducing the aldehyde group into 1,4-position with the aromatic nitrogen atom (Scheme 2). Besides, substituted triazoles find numerous applications in pharmaceuticals, supramolecular chemistry, organic synthesis, chemical biology and industry [23-28]. Moreover, compounds containing 1,2,3-triazole moiety showed a wide spectrum of biological activity [29] including antitubercular [30], antibacterial [31] antimalarial [32], anti-HIV [33], anticancer [34], antiallergic [35], antifungal [36] etc.

A series of aldehydes with triazole fragment was prepared by recently described procedures [37,38] (Scheme 3).

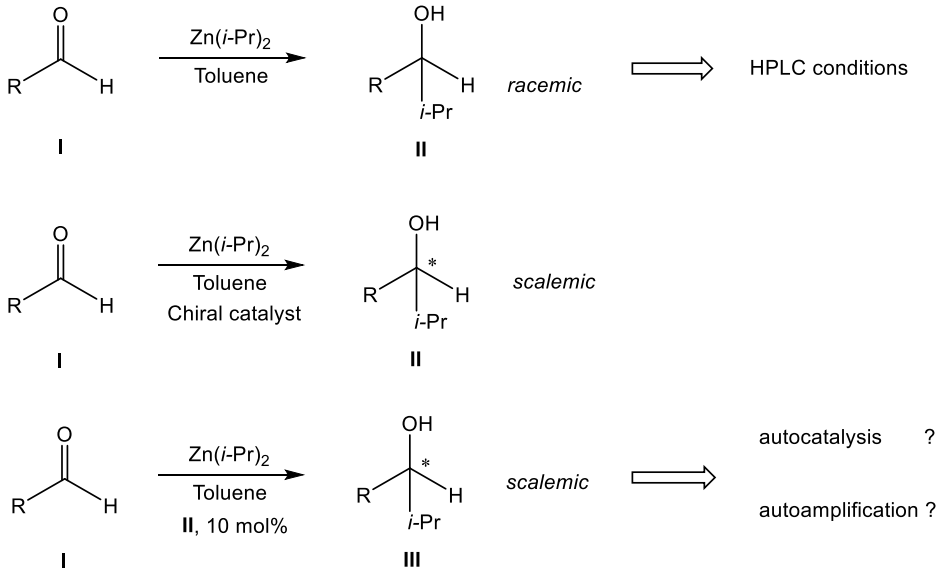

Scheme 1. Trial sequence for searching perspective compounds for autoamplification.

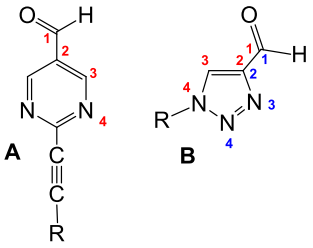

Scheme 2. Comparison of the general formula of Soai aldehydes (**A**) and perspective 1,2,3-triazoles (**B**).

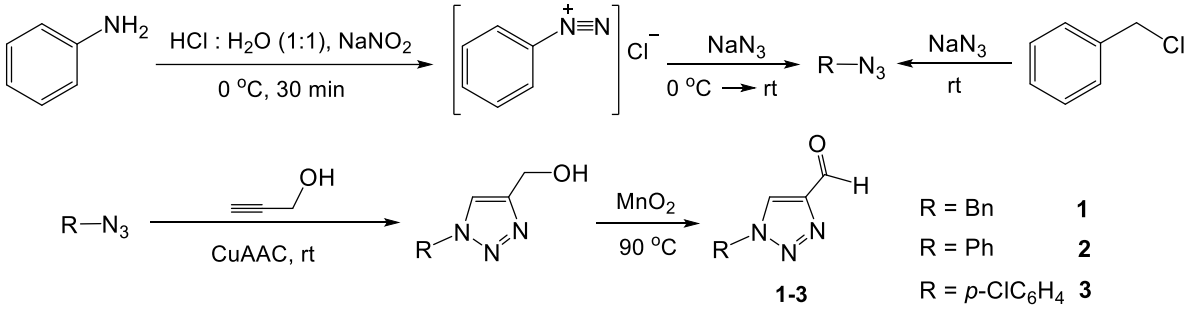

Scheme 3. Synthesis of substituted 1,2,3-triazole aldehydes **1-3**.

3.3. Reactions of compounds 1-3 with diisopropylzinc

Compounds **1-3** react with excess of diisopropylzinc in the presence of a chiral catalyst or without any catalyst (Scheme 4, Table 1).

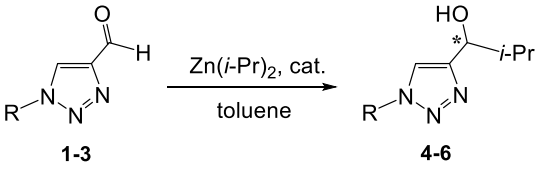

Scheme 4. Catalytic reactions of compounds **1-3** with diisopropyl zinc

Table 1. Reactions of compounds **1-3** with diisopropyl zinc

Entry	Compound number	cat	Ratio Ald : Zn(*i*-Pr)$_2$: cat	Conditions	Yield, %	ee, %
1	**R = Bz (1)**	none	1 : 10	r.t., 4 h	43	3
2			1 : 10	reflux 0.1 h (NMR tube)	25	41
3		Ephedrine[a]	1 : 10 : 0.2	80°C, 6 h	20	35
4			1 : 10 : 0.1	80°C, 4 h	33	37
5			1 : 10 : 0.1	reflux, 0.1 h (NMR tube)	29	10
6		(*R*,*R*)-QiunoxP*[b]	1 : 10 : 0.1	80°C, 4 h	25	2
7		(*R*,*R*)-BenzP*[c]	1 : 10 : 0.1	80°C, 4 h	30	20
8		**1**, 20% ee	1 : 10 : 0.2	r.t., overnight	11	0

9		**1**, 37% ee	1 : 10 : 0.2	80°C, 4 h	30	25
10	**R = Ph (2)**	none	1 : 10	r.t., 4 h	48	0
11		Ephedrine[a]	1 : 10 : 0.1	r.t., 1 h	40	27
12		(*R*,*R*)-QiunoxP*[b]	1 : 10 : 0.1	r.t., 1 h	75	2
13		(*R*,*R*)-BenzP*[c]	1 : 10 : 0.1	r.t., overnight	24	13
14		(–)Sparteine[d]	1 : 10 : 0.1	r.t., 4 h	13	3
15		**2**, 13% ee	1 : 10 : 0.2	r.t., 3 h	48	0
16		**2**, 27% ee	1 : 10 : 0.2	r.t., overnight	47	0
17	**R = *p*-ClC$_4$H$_6$ (3)**	none	1 : 10	r.t., 4 h	37	10
18			1 : 10	r.t., overnight	52	11
19			1 : 10	reflux, 0.1 h (NMR tube)	21	0
20		Ephedrine[a]	1 : 20 : 0.1	r.t., overnight	31	33
21		(*R*,*R*)-QiunoxP*[b]	1 : 10 : 0.1	reflux, 0.1 h (NMR tube)	25	15
22		(*R*,*R*)-BenzP*[c]	1 : 10 : 0.1	reflux, 0.1 h (NMR tube)	20	9
23		**3,** 33% ee	1 : 10 : 0.2	r.t., overnight	53	5

[a]Ephedrine [b](*R*,*R*)-QiunoxP* [c](*R*,*R*)-BenzP* [d](-)Sparteine

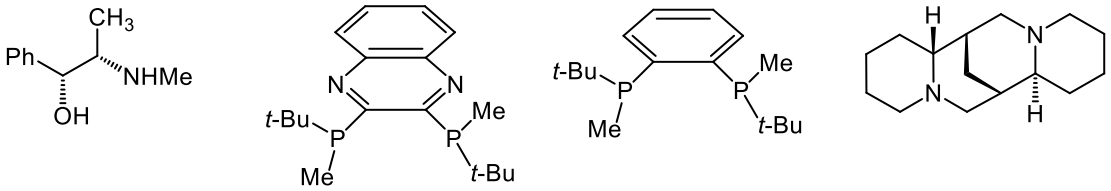

Analysis of the experimental data collected in the Table 1 leads to the following conclusions:

- Significant accelerating effect of a catalyst was observed only in the reaction of **2** catalyzed by (*R,R*)-QuinoxP* (entry 12). For **1** and **3** the highest yields were obtained in the non-catalyzed reactions (entries 1, 18).
- Among applied chiral catalysts only ephedrine leads to the formation of notably optically enriched products (entries 3-5, 11, 20). Even in these cases a negative non-linear effect is observed, since the ee of the products are significantly lower than the ee of the catalyst.
- Autocatalysis was not observed: compare the entries 1 and 8; 10 and 15, 16; 17, 18 and 23.
- Some of the results of the autocatalytic reactions roughly correspond to preserving the ee of the catalyst diluted by a larger amount of the non-chiral product (entries 8, 22). Other results indicate dissipation of chirality (entries 8, 15, 16, 23).
- Spontaneous chirality generation was observed for the substrates **1** and **3** (entries 1, 2, 17, 18).

We assumed that these findings might be a result of different mechanisms operating under dissimilar reaction conditions. We leave the accurate elucidation of these conditions, extending the scope of the substrates, experimental studies of the reaction pools and kinetic simulations for a full paper. In this preliminary communication we would like to

perform a Demonstration of Principle by locating computationally probable catalysts in the reaction pool capable for exhibiting either positive or negative non-linear effects in one of the reactions under study. The former species might be operative in the synthetic protocol resulting in the spontaneous generation of chirality, whereas the latter one might be responsible for the dissipation of the enantiomeric excess in the reactions with the pre-formed catalyst.

3.4. Computational analysis of the reaction of the aldehyde 3 with diisopropyl zinc

A primary product of the alkylation of the aldehyde **3** is alcoholate **7** (Scheme 5). From the previous studies it is known that similar alcoholates readily form oligomers that play an important role in the autocatalysis. We have computed possible oligomerization pathways for **7**.

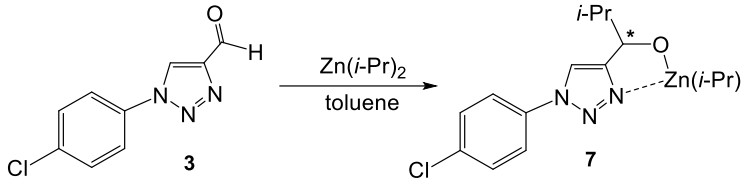

Scheme 5. Formation of monomeric alcoholate **7**.

Similarly to the previously studied cases [9,39], the dimerization of **7** is strongly exogonic and leads to the formation of the square dimers **8**(*SS*) and **8**(*RS*). However, unlike the previous cases, in which the stabilities of the homo- and heterochiral dimers where practically equal, **8**(*RS*) was computed to be more stable than **8**(*SS*) for 3.0 kcal/mol (Scheme 6).

The greater stability of **8**(*RS*) is due to a larger number of CH···HC interactions across the Zn_2O_2 square (Figure 1) arising due to conformational restrictions created by the coordination binding of Zn with the nitrogen atoms in the position 2 of the triazolic rings.

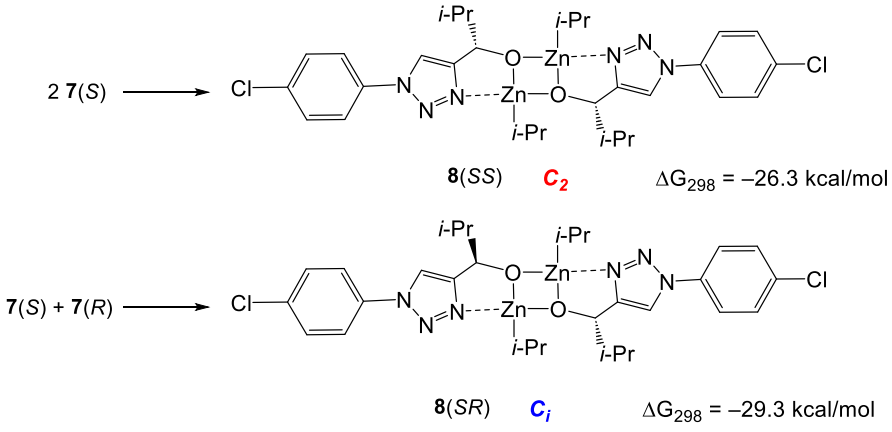

Scheme 6. Formation of square dimers **8**(*SS*) and **8**(*SR*).

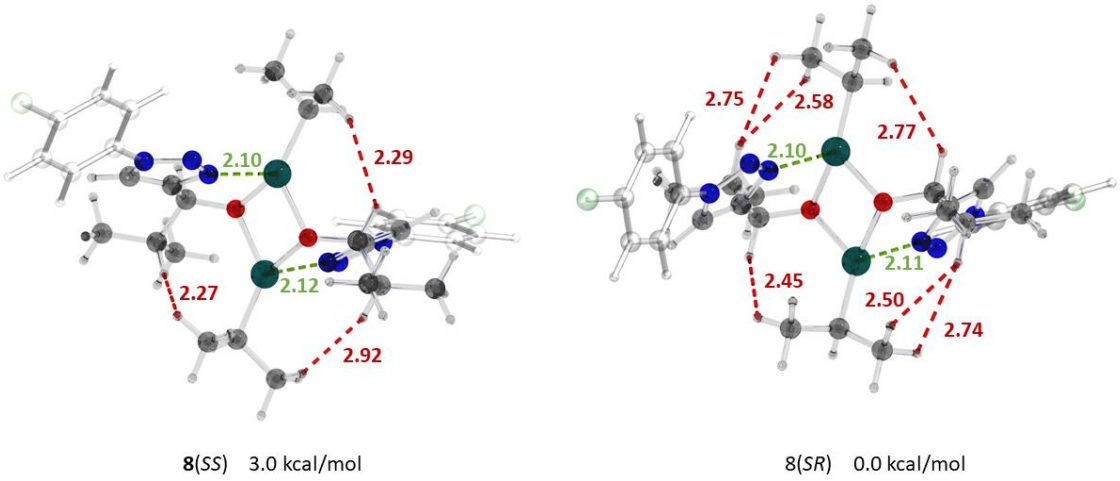

Figure 1. Optimized structures, important interatomic distances (Å) and relative Gibbs free energies (298K) of the square dimers **8**(*SS*) and **8**(*SR*). Atoms: grey – carbon; light grey – hydrogen; red – oxygen; blue – nitrogen; green – chlorine; turquoise – zinc. Interatomic distances: red – CH···HC; green – Zn–N.

Importantly, the significantly higher stability of the heterochiral dimer **8**(*SR*) implies a possibility of a positive NLE via so-called "reservoir effect". It means that the catalyst is a monomer capable for catalyzing an enantioselective reaction, and the minor enantiomer is deactivated via accumulating in the more stable dimer [11]. We investigated this possibility computationally (Scheme 7).

Diisopropyl zinc coordinates in a chelate way to the oxygen and N(2) atoms of **7**(*S*) yielding adduct **9**(*S*). Aldehyde **3** coordinates to the Zn atom, and the following alkyl group transfer via **TS1**(*S*) results in the formation of the adduct **7**(*S*) • **7**(*S*), thus completing an amplifying catalytic cycle.

Similar reaction leading to the opposite enantiomer of the product is possible via the **TS1**(*R*) which is however 7.2 kcal/mol less stable than **TS1**(*S*) due to the significantly smaller number of stabilizing weak interactions between the substrate and the catalyst compared to the **TS1**(*S*) (see Fig. 2).

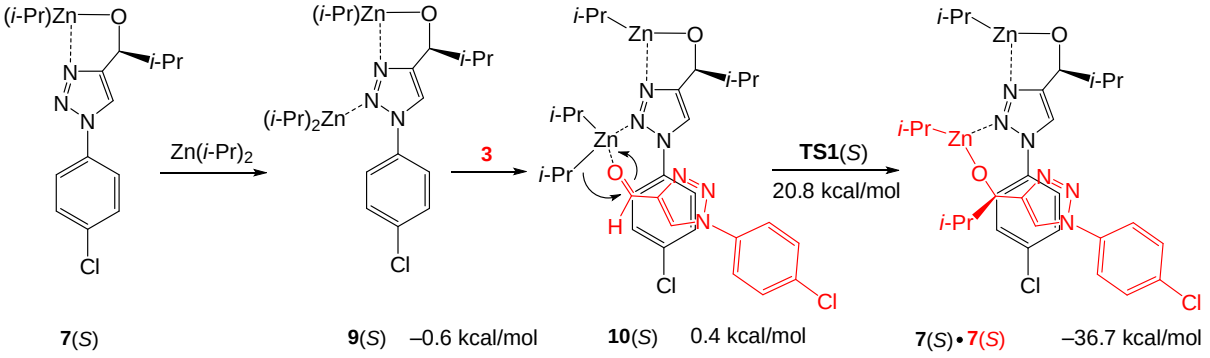

Scheme 7. Computational results (ΔG_{298}, relative to **7**(*S*) + Zn(*i*-Pr)$_2$ + **3**) for the reaction of diisopropyl zinc with aldehyde **3** catalyzed by **7**(*S*). AAA via monomer mechanism.

Thus, we concluded that the AAA is possible for the compound **7** via the "reservoir" mechanism through the combination of the greater stability of the heterochiral dimer

8(*SR*) compared to **8**(*SS*) and the enantioselective alkylation catalyzed by the monomeric alcoholate.

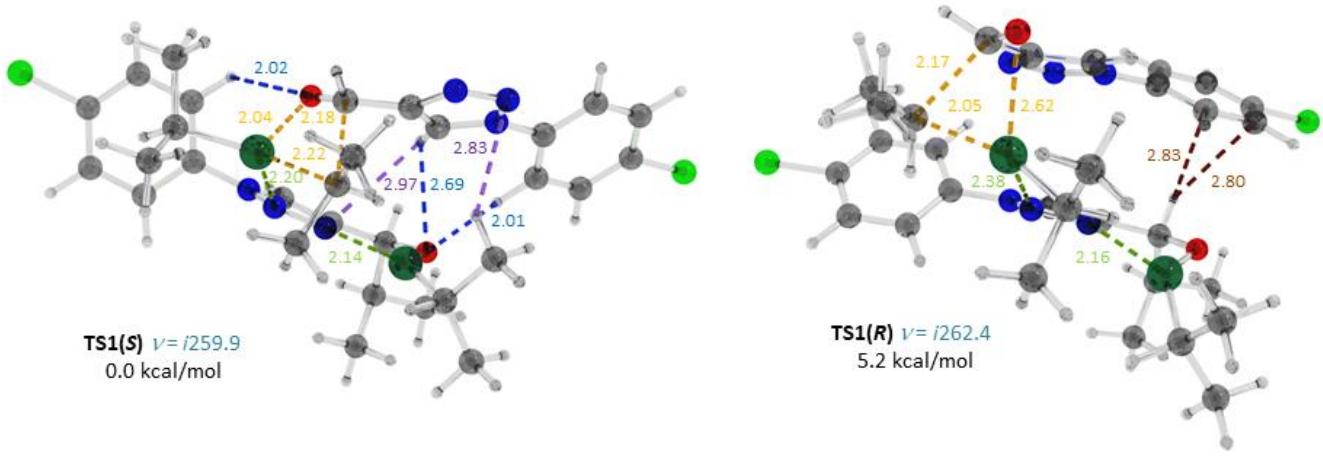

Figure 2. Optimized structures, important interatomic distances (Å) and relative Gibbs free energies of the transition states **TS1**(*S*) and **TS1**(*R*). Atoms: grey – carbon; light grey – hydrogen; red – oxygen; blue – nitrogen; green – chlorine; turquoise – zinc. Interatomic distances: yellow – forming bonds and those being broken; green – Zn–N; blue: CH···O; violet, CH···N; brown – CH···π.

It is evident that very similar transition states can be found for the reactions catalyzed by the resting state species, *i.e.* square dimers **8** (*e.g.* Fig. 3). In that case the reservoir effect is absent and the enantiomeric pairs, **8**(*SS*), **8**(*RR*) and **8**(*SR*), **8**(*RS*) would do exactly the same job producing preferentially the opposite enantiomers, and neither amplifying nor dissipating effects are expected. This mechanism would correlate with the experimental results from the entries 9 and 22 (Table 1).

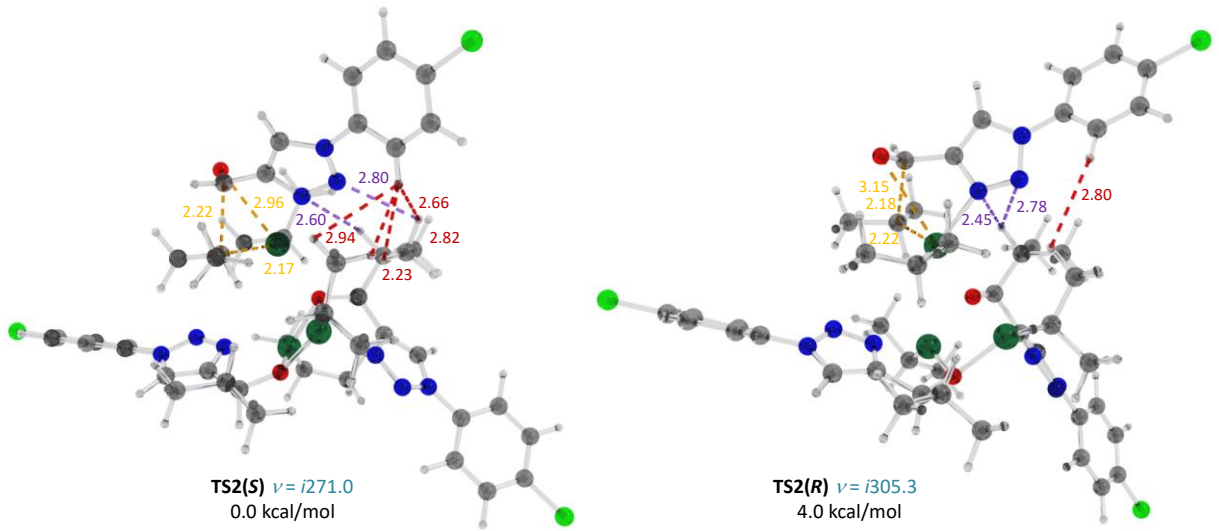

Figure 3. Optimized structures, important interatomic distances (Å) and relative Gibbs free energies of the transition states **TS2**(*S*) and **TS2**(*R*) for the alkylation of **3** catalyzed with **8**(*SS*). Atoms: grey – carbon; light grey – hydrogen; red – oxygen; blue – nitrogen; green – chlorine; turquoise – zinc.

Interatomic distances: yellow – forming bonds and those being broken; green – Zn–N; blue: CH···O; violet, CH···N; red – CH···HC.

Smaller size of the 5-membered heterocycle compared to the pyrimidine or pyridine rings in the classic Soai substrates does not allow creating a 12-membered macrocycle as a core of the tetrameric cluster. Instead a 10-membered ring is formed by one coordination N–Zn bond and one hydrogen O–H bond (Scheme 8).

As a result, only one Zn atom in the core remains capable of coordinating Zn(*i*-Pr)$_2$ yielding **12**(*SSSS*). Either of the 2 *i*-Pr groups of Zn(*i*-Pr)$_2$ can participate in the alkylation (Figure 4). In this case a preferential formation of the opposite enantiomer **7**(*R*) from **8**(*SSSS*)) was computed. The π-π stacking due to the practically coplanar orientation of the incoming aldehyde with one of the alcoholate units of the tetramer in the **TS3**(*R*) makes it significantly more stable than the **TS3**(*S*). Although it is evident that **8**(*RRRR*) would generate **7**(*S*) with the same efficiency, a simple analysis shows that in that situation any existing enantiomeric excess will be degraded to microscopic values. This prediction corresponds to the experimental results from the entries 8, 15, 16 and 21 in the Table 1.

4. Discussion

Our computational results based on the preliminary experimental findings testify that in the reaction of diisopropyl zinc with triazoles **1-3** three different regimes of the ee changes in the course of the reaction: accumulation to the detectable amounts, keeping the microscopic ee unchanged and degradation of the macroscopic ee to microscopic values.

This situation must be a much more frequent compared to the perfect Asymmetri Auto Amplification in the Soai Reaction. On the other hand, the evidently increasing randomness of the chiral amplification makes its observation and proper characterization significantly more difficult.

We realize that a much larger set of experimental data would be necessary for claiming achievement of some control over the AAA. Extension of the substrates scope, serial experiments, NMR studies of the reaction pools of these reactions as well as kinetic simulations based on the computed catalytic cycles are in progress in our laboratories.

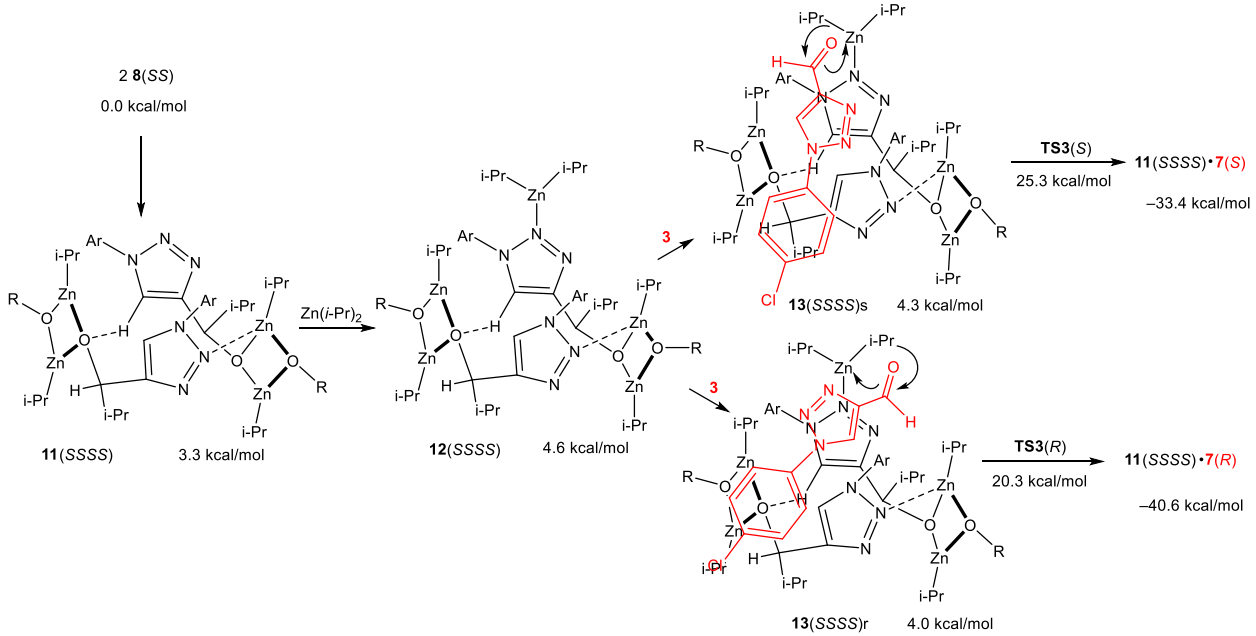

Scheme 8. Computational results (ΔG$_{298}$, relative to 2 **8**(*S*) + Zn(*i*-Pr)$_2$ + **3**) for the reaction of diisopropyl zinc with aldehyde **3** catalyzed by **7**(*S*). AAA via monomer mechanism.

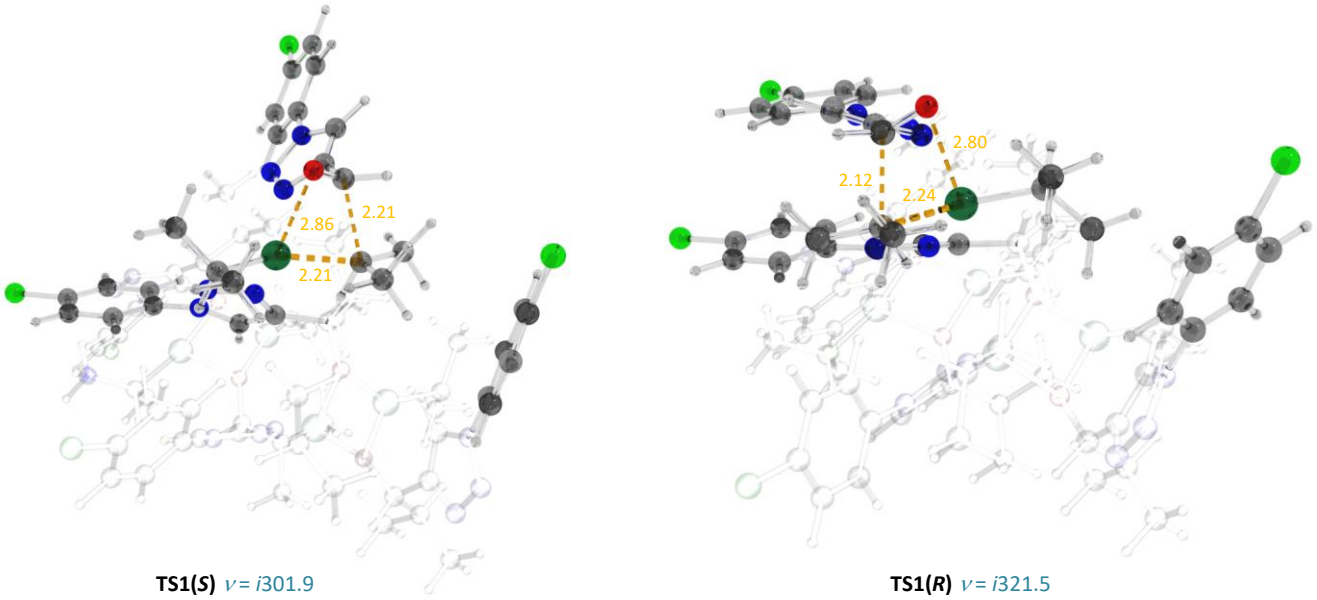

Figure 4. Optimized structures, important interatomic distances (Å) and relative Gibbs free energies of the transition states **TS2**(*S*) and **TS2**(*R*) for the alkylation of **3** catalyzed with **8**(*SS*). Atoms: grey – carbon; light grey – hydrogen; red – oxygen; blue – nitrogen; green – chlorine; turquoise – zinc. Interatomic distances: yellow – forming bonds and those being broken.

Supplementary Materials: The following supporting information can be downloaded at: www.mdpi.com/xxx/s1, experimental details, NMR and HPLC charts, computational details.

Author Contributions: Conceptualization, I.D.G. and A.R.K.; investigation, O.A.M., L.Z.L and E.Sh.S.; writing—original draft preparation, I.D.G.; writing—review and editing, A.R.K.; supervision, I.D.G.; project administration, I.D.G.; funding acquisition, I.D.G. All authors have read and agreed to the published version of the manuscript.

Funding: This research was funded by a Research Grant from Russian Science Foundation #22-13-00275.

Conflicts of Interest: The authors declare no conflict of interest.

References

1. Soai, K.; Shibata, T.; Morioka, H.; Choji, K. Asymmetric autocatalysis and amplification of enantiomeric excess of a chiral molecule. *Nature* **1995**, *378*, 767–768.
2. Mislow, K. Absolute asymmetric synthesis: A commentary. *Collect. Czech. Chem. Commun.* **2003**, *68*, 849–864.
3. Soai, K. Asymmetric Autocatalysis, Absolute Asymmetric Synthesis and Origin of Homochirality of Biomolecules. In: "*Progress in Biological Chirality*"; Palyi, G., Zucchi, C., Caglioti, L., Eds.; Elsevier: London, UK, **2004**; Volume 1, pp 355–364.
4. Brown, J.M. Reaction Mechanism in the Study of Amplifying Asymmetric Autocatalysis. In: "*Asymmetric Autocatalysis: The Soai Reaction*"; Soai, K., Kawasaki, T., Matsumoto, A., Eds.; Royal Society of Chemistry: Cambridge, UK, **2022**; Volume 43, pp 97–128.
5. Soai, K; Sato, I.; Shibata, T.; Komiya, S.; Hayashi, M.; Matsueda, Y.; Imamura, H.; Hayase, T.; Morioka, H.; Tabira, H.; Yamamoto, J.; Kowata, Y. Asymmetric synthesis of pyrimidyl alkanol without adding chiral substances by the addition of diisopropylzinc to pyrimidine-5-carbaldehyde in conjunction with asymmetric autocatalysis. *Tetrahedron: Asymmetry* **2003**, *14*, 185–188.
6. Gridnev, I.D.; Serafimov, J.M.; Quiney, H.; Brown, J.M. Reflections on spontaneous asymmetric synthesis by amplifying autocatalysis. *Org. Biomol. Chem.* **2003**, *1*, 3811–3819.
7. Singleton, D.A; Vo, L.K. A Few Molecules Can Control the Enantiomeric Outcome. Evidence Supporting Absolute Asymmetric Synthesis Using the Soai Asymmetric Autocatalysis. *Org. Lett.* **2003**, *23*, 4337–4339.
8. Soai, K.; Shibata, T.; Sato, I. Discovery and Development of Asymmetric Autocatalysis. *Bull. Chem. Soc. Jpn.* **2004**, 77, 1063–1073.

9. Gridnev, I.D.; Vorob'ev, A.Kh. Quantification of Sophisticated Equilibria in the Reaction Pool and Amplifying Catalytic Cycle of the Soai Reaction. *ACS Catalysis* **2012,** *2*, 2137–2149.
10. Athavale, S.V.; Simon, A.; Houk, K.N.; Denmark, S.E. Structural Contributions to Autocatalysis and Asymmetric Amplification in the Soai Reaction. *J. Am. Chem. Soc.* **2020**, *142*, 18387–18406.
11. Girard, C.; Kagan, H.B. Nonlinear Effects in Asymmetric Synthesis and Stereoselective Reactions: Ten Years of Investigation. *Angew. Chem. Int. Ed.* **1998**, *37*, 2922–2959.
12. Chai, J.-D.; Head-Gordon, M. Long-Range Corrected Hybrid Density Functionals with Damped Atom–Atom Dispersion Corrections. *Phys. Chem. Chem. Phys.* **2008**, *10*, 6615–6620.
13. Frisch, M. J.; Trucks, G. W.; Schlegel, H. B.; Scuseria, G. E.; Robb, M. A.; Cheeseman, J. R.; Scalmani, G.; Barone, V.; Mennucci, B.; Petersson, G. A.; Nakatsuji, H.; Caricato, M.; Li, X.; Hratchian, H. P.; Izmaylov, A. F.; Bloino, J.; Zheng, G.; Sonnenberg, J. L.; Hada, M.; Ehara, M.; Toyota, K.; Fukuda, R.; Hasegawa, J.; Ishida, M.; Nakajima, T.; Honda, Y.; Kitao, O.; Nakai, H.; Vreven, T.; Montgomery, J. A., Jr.; Peralta, J. E.; Ogliaro, F.; Bearpark, M.; Heyd, J. J.; Brothers, E.; Kudin, K. N.; Staroverov, V. N.; Kobayashi, R.; Normand, J.; Raghavachari, K.; Rendell, A.; Burant, J. C.; Iyengar, S. S.; Tomasi, J.; Cossi, M.; Rega, N.; Millam, J. M.; Klene, M.; Knox, J. E.; Cross, J. B.; Bakken, V.; Adamo, C.; Jaramillo, J.; Gomperts, R.; Stratmann, R. E.; Yazyev, O.; Austin, A. J.; Cammi, R.; Pomelli, C.; Ochterski, J. W.; Martin, R. L.; Morokuma, K.; Zakrzewski, V. G.; Voth, G. A.; Salvador, P.; Dannenberg, J. J.; Dapprich, S.; Daniels, A. D.; Farkas, O.; Foresman, J. B.; Ortiz, J. V.; Cioslowski, J.; Fox, D. J. Gaussian 09, rev. D.01; Gaussian, Inc.: **2013**.
14. Becke, A. D. Density-functional exchange-energy approximation with correct asymptotic behavior. *Phys. Rev. A* **1988**, *38*, 3098– 3100.
15. Ditchfield, R.; Hehre, W. J.; Pople, J. A. Self-Consistent Molecular-Orbital Methods. IX. An Extended
16. Gaussian-Type Basis for Molecular-Orbital Studies of Organic Molecules. *J. Chem. Phys.*,**1971**, *54*, 724-728.
17. Hehre, W. J.; Ditchfield, R.; Pople, J. A. Self-Consistent Molecular Orbital Methods. XII. Further Extensions of Gaussian-Type Basis Sets for Use in Molecular Orbital Studies of Organic Molecules *J. Chem. Phys*., **1972**, *56*, 2257-2261.
18. Hariharan, P. C.; Pople, J. A. The influence of polarization functions on molecular orbital hydrogenation energies. *Theor. Chim. Acta*, **1973**, *28*, 213-222.
19. Francl, M. M.; Pietro, W. J.; Hehre, W. J.; Binkley, J. S.; Gordon, M. S.; DeFrees, D. J.; Pople, J. A. Self-consistent molecular orbital methods. XXIII. A polarization-type basis set for second-row elements. *J. Chem. Phys.* **1982**, *77*, 3654-3665.
20. Gordon, M. S.; Binkley, J. S.; Pople, J. A.; Pietro, W. J.; Hehre, W. J. Self-consistent molecular-orbital methods. Small split-valence basis sets for second-row elements. *J. Am. Chem. Soc. 1982*, **104**, 2797-2803.
21. Rassolov, V. A.; Pople, J. A.; Ratner, M. A.; Windus, T. L. 6-31G * basis set for atoms K through Zn. *J. Chem. Phys.* **1998**, *109*, 1223-1229.
22. Marenich, A. V.; Cramer, C. J.; Truhlar, D. G. Universal Solvation Model Based on Solute Electron Density and on Continuum Model of the Solvent Defined by the Bulk Dielectric Constant and Atomic Surface Tensions. *J. Phys. Chem. B* **2009**, *113*, 6378-6396.
23. Dheer, D.; Singh, V.; Shankar, R. Medicinal attributes of 1,2,3-triazoles: Current developments. *Bioorg. Chem.* **2017**, *71*, 30–54.
24. Schulze, B.; Schubert, U.S. Beyond click chemistry–Supramolecular interactions of 1,2,3-triazoles. *Chem. Soc. Rev.* **2014**, *43*, 2522–2571.
25. Liang, L.; Astruc, D. The copper (I)-catalyzed alkyne-azide cycloaddition (CuAAC) "click" reaction and its applications. An overview. *Coord. Chem. Rev.* **2011**, 255, 2933–2945.
26. Ngo, J.T.; Adams, S.R.; Deerinck, T.J.; Boassa, D.; Rodriguez-Rivera, F.; Palida, S.F.; Bertozzi, C.R.; Ellisman, M.H.; Tsien, R.Y. Click-EM for imaging metabolically tagged nonprotein biomolecules. *Nat. Chem. Biol.* **2016**, *12*, 459–465.
27. Astruc, D.; Liang, L.; Rapakousiou, A.; Ruiz, J. Click dendrimers and triazole-related aspects: Catalysts, mechanism, synthesis, and functions. A bridge between dendritic architectures and nanomaterials. *Acc. Chem. Res.* **2012**, *45*, 630–640.
28. Wang, X.; Huang, B.; Liu, X.; Zhan, P. Discovery of bioactive molecules from CuAAC click-chemistry-based combinatorial libraries. *Drug Discov. Today* **2016**. *21*. 118–132.
29. Bozorov, K.; Zhao, J.; Aisa, H.A. 1,2,3-Triazole-containing hybrids as leads in medicinal chemistry: A recent overview. *Bioorg. Med. Chem.* **2019**, *27*, 3511−3531.
30. Zhang, S.; Xu, Z.; Gao, C.; Ren, Q.C.; Chang, L.; Lv, Z.S.; Feng, L.S. Triazole derivatives and their anti-tubercular activity. *Eur. J. Med. Chem.* **2017**, *138*, 501−513.
31. Bangalore, P.K.; Vagolu, S.K.; Bollikanda, R.K.; Veeragoni, D.K.; Choudante, P.C.; Misra, S.; Sriram, D.; Sridhar, B.; Kantevari, S. Usnic Acid Enaminone-Coupled 1, 2, 3-Triazoles as antibacterial and antitubercular Agents. *J. Nat. Prod.* **2019**, *83*, 26−35.
32. Manohar, S.; Khan, S. I.; Rawat, D. S. Synthesis of 4-aminoquinoline-1, 2, 3-triazole and 4-aminoquinoline-1, 2, 3-triazole-1, 3, 5-triazine hybrids as potential antimalarial agents. Chem. *Biol. Drug Des.* **2011**, *78*, 124−136.
33. Pribut, N.; Veale, C.G.L.; Basson, A.E.; van Otterlo, W.A.L.; Pelly, S.C. Application of the Huisgen cycloaddition and 'click' reaction toward various 1, 2, 3-triazoles as HIV non-nucleoside reverse transcriptase inhibitors. *Bioorg. Med. Chem. Lett.* **2016**, *26*, 3700−3704.

34. Narsimha, S.; Nukala, S.K.; Jyostna, T.S.; Ravinder, M.; Rao, M.S.; Reddy, N.V. One-pot synthesis and biological evaluation of novel 4-[3-fluoro-4-(morpholin-4-yl)] phenyl-1*H*-1,2,3-triazole derivatives as potent antibacterial and anticancer agents. *J. Heterocyclic Chem.* **2020**, *57*, 1655−1665.
35. Buckle, D.R.; Outred, D.J.; Rockell, C.J.M.; Smith, H.; Spicer, B.A. Studies on v-triazoles. 7. Antiallergic 9-oxo-1*H*, 9*H* benzopyrano[2, 3-d]-v-triazoles. *J. Med. Chem.* **1983**, *26*, 251−254.
36. Kant, R.; Kumar, D.; Agarwal, D.; Gupta, R.D.; Tilak, R.; Awasthi, S.K.; Agarwal, A. Synthesis of newer 1,2,3-triazole linked chalcone and flavone hybrid compounds and evaluation of their antimicrobial and cytotoxic activities. *Eur. J. Med. Chem.* **2016**, *113*, 34–49.
37. Song, H.; Rogers, N.J.; Brabec, V.; Clarkson, G.J.; Coverdale, J.P.C.; Kostrhunova, H.; Phillips, R.M.; Postings, M.; Shepherd, S.L.; Scott P. Triazole-based, optically-pure metallosupramolecules; highly potent and selective anticancer compounds *Chem. Commun.* **2020**, *56*, 6392–6395.
38. Dai, Z.C.; Chen, Y.F.; Zhang, M.; Li, S.K. Yang, T.-T.; Shen, L.; Wang, J.X.; Qian, S.S.; Zhu, H.L.; Ye, Y.H. Synthesis and antifungal activity of 1,2,3-triazole phenylhydrazone derivatives *Org.Biomol. Chem.* **2015**, *13*, 477–486.
39. Gridnev, I.D.; Serafimov, J.M.; Brown, J.M. Solution Structure and Reagent Binding of the Zinc Alkoxide Catalyst in the Soai Asymmetric Autocatalytic Reaction. *Angew. Chem. Int. Ed.* **2004**, *43*, 4884–4887.